JOURNAL OF VIROLOGY, Apr. 2010, p. 3962–3973 Vol. 84, No. 8
0022-538X/10/$12.00 doi:10.1128/JVI.02291-09

A Novel Inhibitor of the NF-κB Signaling Pathway Encoded by the Parapoxvirus Orf Virus▽

D. G. Diel,[1,2] G. Delhon,[3] S. Luo,[1] E. F. Flores,[2] and D. L. Rock[1]*

Department of Pathobiology, College of Veterinary Medicine, University of Illinois, Urbana, Illinois[1]; Programa de Pós-graduação em Medicina Veterinária, Setor de Virologia, Departamento de Medicina Veterinária Preventiva, Centro de Ciências Rurais, Universidade Federal de Santa Maria, RS, Brazil[2]; and Department of Veterinary and Biomedical Sciences, and Nebraska Center for Virology, University of Nebraska-Lincoln, Lincoln, Nebraska[3]

Received 29 October 2009/Accepted 29 January 2010

The parapoxvirus orf virus (ORFV) is a pathogen of sheep and goats that has been used as a preventive and therapeutic immunomodulatory agent in several animal species. However, the functions (genes, proteins, and mechanisms of action) evolved by ORFV to modulate and manipulate immune responses are poorly understood. Here, the novel ORFV protein ORFV024 was shown to inhibit activation of the NF-κB signaling pathway, an important modulator of early immune responses against viral infections. Infection of primary ovine cells with an *ORFV024* deletion mutant virus resulted in a marked increase in expression of NF-κB-regulated chemokines and other proinflammatory host genes. Expression of ORFV024 in cell cultures significantly decreased lipopolysaccharide (LPS)- and tumor necrosis factor alpha (TNF-α)-induced NF-κB-responsive reporter gene expression. Further, ORFV024 expression decreased TNF-α-induced phosphorylation and nuclear translocation of NF-κB-p65, phosphorylation, and degradation of IκBα, and phosphorylation of IκB kinase (IKK) subunits IKKα and IKKβ, indicating that ORFV024 functions by inhibiting activation of IKKs, the bottleneck for most NF-κB activating stimuli. Although ORFV024 interferes with activation of the NF-κB signaling pathway, its deletion from the OV-IA82 genome had no significant effect on disease severity, progression, and time to resolution in sheep, indicating that ORFV024 is not essential for virus virulence in the natural host. This represents the first description of a NF-κB inhibitor encoded by a parapoxvirus.

Orf virus (ORFV) is the type member of *Parapoxvirus*, one of the eight genera of the subfamily *Chordopoxvirinae* of the *Poxviridae* (43). Other members of the genus include bovine papular stomatitis virus (BPSV), pseudocowpox virus, and parapoxvirus of red deer in New Zealand (43). Parapoxviruses are characterized by the ovoid shape of virions, the presence of criss-cross-arranged surface tubulelike structures, and the high G+C content of their genomes (21).

ORFV is the causative agent of orf (contagious ecthyma, contagious pustular dermatitis, or scabby mouth), a nonsystemic, highly contagious, ubiquitous disease of sheep and goats which is characterized by maculopapular and proliferative lesions affecting the skin around the mouth, nostrils and teats, and the oral mucosa (29). Lesions are largely confined to areas surrounding the virus entry sites, evolving through stages of erythema, vesicles, pustules, and scabs (21). In the absence of secondary infections, lesions are usually resolved in 6 to 8 weeks; however, persistent infections have been reported (13, 27, 48). Orf primarily affects animals less than 1 year old, and morbidity in a susceptible flock may reach 90%. Mortality is usually low; however, lesions in lips and udders may prevent affected animals from suckling, which can result in rapid emaciation (39). In spite of a vigorous and typical antiviral T-helper type 1 (Th1) immune response, immunity elicited by ORFV is short-lived, and animals can be repeatedly infected, albeit lesions are smaller and resolve sooner than in primary infections (28, 40, 69). Orf is a zoonotic disease, affecting humans in close contact with infected animals (17, 44, 55).

The ORFV genome is approximately 138 kbp, with a G+C content of 64%, and contains 131 putative genes, 89 of which are conserved in all characterized chordopoxviruses (14, 61). Based on sequence homology to host and viral genes, several immunomodulatory genes with putative virulence functions have been identified in ORFV, including a homologue of interleukin-10 (IL-10; *ORFV127*), chemokine binding protein (*ORFV112*), inhibitor of granulocyte-macrophage colony-stimulating factor and IL-2 (GIF; *ORFV117*), vascular endothelial growth factor (*ORFV132*), and interferon (IFN) resistance gene (*ORFV020*) (reviewed in reference 21). Recently, screening of vaccinia virus-orf virus recombinants led to identification of a Bcl-2-like inhibitor of apoptosis (*ORFV125*) (66). Notably, ORFV encodes 15 mostly terminally located genes, which lack similarity to other poxvirus or cellular proteins and with putative virulence and host range functions (14).

Historically, ORFV has been used in veterinary medicine as a preventive and therapeutic immunomodulatory agent (reviewed in reference 64). Live or inactivated ORFV preparations exhibit dose-dependent immunomodulatory effects, with therapeutic efficacy and a favorable side effect profile demonstrated for various diseases, including infectious diseases of companion and farm animals (5, 7, 18, 19, 38, 70). Inactivated ORFV has been shown to induce an autoregulatory cytokine

* Corresponding author. Mailing address: 2522 Veterinary Medicine Basic Science Building, University of Illinois, MC-002, 2001 S. Lincoln Avenue, Urbana, IL 61802. Phone: (217) 333-2449. Fax: (217) 244-7421. E-mail: dlrock@illinois.edu.

▽ Published ahead of print on 10 February 2010.

response in mice, involving upregulation of Th1-type cytokines (IL-12, IL-18, and IFN-γ) and their subsequent downregulation, which is accompanied by the induction of IL-10 and IL-4 (64). In addition, inactivated ORFV promotes activation of monocytes and dendritic cells via Toll-like receptor (TLR)-dependent and independent pathways, leading to the synthesis and release of early proinflammatory cytokines (22, 60). Currently, ORFV functions (genes, proteins, and mechanisms of action) associated with modulation and manipulation of early host immune responses are poorly understood.

Many viruses, including hepatitis C virus, paramyxoviruses, influenza virus, African swine fever virus, and poxviruses, encode for proteins that disrupt or modulate immune responses by targeting specific aspects of the nuclear factor κB (NF-κB) signaling pathway (reviewed in references 31 and 63). By binding to specific promoter sequences, NF-κB mediate expression of a wide variety of cellular genes, including many involved in innate immunity, inflammation, and apoptosis, which are critical for early antiviral responses (31, 52, 57, 63). The activity of NF-κB is regulated by its association with the inhibitory IκB molecules, which sequester NF-κB in the cytoplasm (33). Various stimuli, including the proinflammatory cytokines tumor necrosis factor alpha (TNF-α) and IL-1, bacterial lipopolysaccharide (LPS), viruses, and viral products, lead to phosphorylation of IκB proteins by IκB kinases, resulting in proteasomal degradation of IκB and nuclear translocation of NF-κB subunits (33). NF-κB subunits are subject to extensive posttranslational modifications, which may facilitate their nuclear translocation or define their transcriptional functions in the nucleus (9, 53). The critical IκB kinase (IKK) complex is the bottleneck for most NF-κB-activating pathways (33, 57), including those initiated at TLRs and TNF receptors (8), and several viruses have evolved strategies to inhibit IKK complex activation (reviewed in reference 56).

Poxviral proteins involved in inhibition of the NF-κB pathway have been identified in members of the genera *Orthopoxvirus*, *Leporipoxvirus*, *Yatapoxvirus*, and *Molluscipoxvirus*, with selected viruses encoding for multiple inhibitors [for a review, see reference 41]. For example, the type member of the *Poxviridae* vaccinia virus (VACV) encodes at least seven NF-κB inhibitors (A52R, A46R, B14, K1L, N1L, M2L, and E3L), which target different steps leading to NF-κB activation, most often by preventing IKK complex activation (11, 15, 24, 30, 46, 59, 62). Notably, deletion of individual genes encoding selected VACV NF-κB inhibitors from the viral genome resulted in various degrees of attenuation in mice. However, no individual gene deletion rendered complete attenuation (2, 10, 30), suggesting that encoded proteins exhibit, to some extent, complementary functions during VACV infection (41).

Homologues of known poxviral NF-κB inhibitors are absent in parapoxviruses, suggesting that either they encode novel NF-κB inhibitors or employ alternative immune evasion strategies. We present data here demonstrating that *ORFV024*, a gene unique to parapoxviruses, profoundly affects chemokine and other proinflammatory gene transcription in infected cells. Expression of ORFV024 in cell cultures decreased the phosphorylation and nuclear translocation of NF-κB-p65, the phosphorylation and degradation of IκBα, and the phosphorylation of IKKα and IKKβ, indicating that ORFV024 expression suppresses early cellular responses to ORFV infection by inhibiting activation of the NF-κB pathway. Notably, *ORFV024* is not essential for viral virulence since its deletion did not affect ORFV pathogenesis in sheep.

MATERIALS AND METHODS

Cells and virus. Primary ovine fetal turbinate (OFTu) cells were kindly provided by Howard D. Lehmkuhl (USDA) and were maintained in minimal essential medium (MEM) supplemented with 10% fetal bovine serum (FBS), 2 mM L-glutamine, 50 μg of gentamicin/ml, 100 U of penicillin/ml, and 100 μg of streptomycin/ml. HeLa cells (American Type Culture Collection) were maintained in Dulbecco modified essential medium supplemented with 10% FBS, 2 mM L-glutamine, 50 μg of gentamicin/ml, 100 U of penicillin/ml, and 100 μg of streptomycin/ml. ORFV strain OV-IA82 was isolated from sheep nasal secretions at the Iowa Ram test Station during an orf outbreak in 1982, and its genome has been fully sequenced (14). Low-passage parental OV-IA82 virus was used to construct the deletion mutant virus OV-IA82Δ024 and in all procedures involving infections with wild-type virus, PCR amplification, and cloning of viral genes.

Plasmids. *ORFV024* coding sequence was PCR amplified from the OV-IA82 genome and cloned into the expression vectors pCMVTag4A (Stratagene, La Jolla, CA) and pEGFP-N1 (Clontech, Mountain View, CA). PCR primers were 024Flag-Fw(HindIII)-5′-TAAGGCCTCTAAGCTTATGGCCTCCTACGTC AGCGGCGCT-3′, 024Flag-Rv(XhoI)-5′-CAGAATTCGCCTCGAGCACG TAGACCGTGTGCGTGCGC-3′, 024EGFP-Fw(XhoI)-5′-ATCTTAGCTC GAGCTAAGATGGCCTCCTAC-3′, and 024EGFP-Rv(HindIII)-5′-CAGAAT AAGCTTCACGTAGACCGTGTGCGTG-3′. The restriction enzymes used for cloning are indicated on each primer. DNA sequencing of constructs confirmed the integrity of *ORFV024* sequence and in-frame cloning of FLAG (pCMV024-Flag) and EGFP (p024EGFP) tag proteins.

For mutant virus generation, a recombination cassette was constructed by PCR amplification of *ORFV024* left (LF; 856 bp) and right (RF; 866 bp) flanking regions from the OV-IA82 genome, followed by cloning of amplicons into vector pZippy-Neo/Gus (16). Primers used for amplification were 024LF-Fw(HindIII)-5′-TAAG GCCTCTAAGCTTAACCAGCAGACCTTCTTCACCAA-3′, 024LF-Rv(SalI)-5′-CAGAATTCGCGTCGACCTTAGCTCTGTCTGAACTGAAGCA-3′, 024RF-Fw(NotI)-5′-ATTCTTATGCGGCCGCGCCGGCTTCATCCGCCGCAGCATA-3′, and 024RF-Rv(BglII)-5′-CAGAATTCGCAGATCTTACGGCGACACCGAC TCCGTGTTC-3′. Restriction enzymes used for cloning are indicated on each primer. The recombination cassette pZ024LF-Neo/Gus-024RF was constructed by cloning *ORFV024* LF and RF flanking regions on each side of a reporter construct consisting of neomycin (Neo) resistance and β-glucuronidase (Gus) genes preceded by VACV VV7.5 and modified H5 promoters, respectively.

ORFV024 sequence alignment. Alignment of ORFV024 was performed using CLUSTAL W (Biology Workbench). Accession numbers of the aligned proteins are AAR98119.1 (OV-IA82), ABA00541.1 (OV-NZ2), AAP76384.1 (OV-Orf11), AAR98249.1 (OV-SA00), AAR98381.1 (BPSV-AR02), and GQ911582 (BPSV-TX-09).

RT-PCR. Transcription kinetics of *ORFV024* was assessed during ORFV infection *in vitro* by reverse transcription-PCR (RT-PCR). OFTu cells were cultured in 35-mm dishes for 16 h and inoculated with the wild-type virus OV-IA82 (multiplicity of infection [MOI] = 10) in the presence or absence of cytosine arabinoside (AraC; 40 μg/ml; Sigma Aldrich, St. Louis, MO) an inhibitor of DNA replication and, consequently, of late poxviral transcription (12). Cells were harvested at 0, 1, 2, 3, 6, 12, and 24 h postinoculation (p.i.), and total RNA was extracted using TRIzol reagent (Invitrogen, San Diego, CA). Samples were treated with DNase I (New England Biolabs, Ipswich, MA) for 10 min at 37°C, and RNA was purified by using the RNeasy minikit (Qiagen, Valencia, CA). A total of 2 μg of RNA was reverse transcribed by using a Superscript III kit (Invitrogen), following the manufacturer's protocol. The oligo(dT) used in RT reactions was oligo-dT-5′-ATGGATGCCTACAGCGCTCTTTTTTTTTTTTTT TTTTTT-3′. *ORFV024*, *ORFV127* (early gene control), and *ORFV055* (late gene control) transcription was assessed by using 1 μl of cDNA and the following primers 024intFw-5′-GCGGACACAGCCACAACCACAGTC-3′, 024intRv-5′-CTAGCACGCGCTTTCGGTACCGCC-3′, 127EintFw-5′-CTCCTCGAC GACTTCAAAGG-3′, 127EintRv-5′-TATGTCGAACTCGCTCATGG-3′, 055LFw-5′-AATCATGGATCCGCCACCATGTTCTTCGCGCGTCGC-3′, and 055LRv-5′-TATCATCTCGAGCGGGCGTGGAGGTCGCCGACC-3′. Negative controls and controls for DNA contamination (no reverse transcriptase) were included in all reactions.

Construction and characterization of *ORFV024* deletion mutant virus OV-IA82Δ024. OV-IA82Δ024 was obtained by homologous recombination between the parental ORFV strain OV-IA82 and the recombination cassette pZ024LF-

Neo/Gus-024RF. OFTu cells cultured in 25-cm^2 flasks were infected with OV-IA82 (MOI = 1) and 3 h later transfected with pZ024LF-Neo/Gus-024RF (10 μg) using Lipofectamine 2000 according to manufacturer's recommendations. At 48 h after infection/transfection, cultures were harvested, and cell lysates were used for selection of recombinant viruses by plaque assay. OFTu cells cultured in six-well plates were infected with serial 10-fold dilutions of cell lysates from the infection/transfection and overlaid with culture medium containing 0.5% SeaKem GTC agarose (Cambrex Bioscience, Rockland, ME) and 5-bromo-4-chloro-3-indolyl-β-D-glucuronic acid (X-Gluc; 0.5 μg/ml, Gold Biotechnologies, St. Louis, MO). Blue plaques indicative of recombination were harvested and subjected to additional rounds of plaque purification. The absence of *ORFV024* sequence and presence of Neo/Gus sequences in the purified recombinant virus were confirmed by PCR and Southern blotting. The primers used for PCR amplification of *ORFV024* and Neo/Gus reporter gene were 024intFw-5′-GCGG ACACAGCCACAACCACAGTC-3′, 024intRv-5′-CTAGCACGCGCTTTCGGT ACCGCC-3′, NG2Fw-5′-ATCAGGACATAGCGTTGGCTACC-3′, and NG2 Rv-5′-TGCCGTAATGAGTGACCGCATCGA-3′, respectively. To assess the integrity of regions involved in recombination, 824 and 874 bp on the left and right flanking regions of *ORFV024* were sequenced by using an Applied Biosystems Prism 3730 X1 automated DNA sequencer (Applied Biosystems, Foster City, CA).

Growth characteristics of deletion mutant virus OV-IA82Δ024 and wild-type virus OV-IA82 were analyzed and compared in primary OFTu cells and in HeLa cells. Multiple step growth curve was performed in OFTu cells inoculated with mutant or wild-type virus (MOI = 0.1), and at 12, 24, 48, and 72 h postinfection (p.i.) viral yields were quantitated in cultures of OFTu cells by the Spearman-Karber's 50% tissue culture infectious dose ($TCID_{50}$) method. One-step growth curves were performed in OFTu and HeLa cells inoculated with mutant or wild-type virus (MOI = 10), and at 6, 12, 24, and 48 h p.i. viral yields were quantitated in cultures of OFTu cells as described above. To compare the cytopathic effect (CPE) induced by OV-IA82Δ024 and OV-IA82, cells were inoculated with each virus (MOI = 10) and 48 h p.i. evaluated under an inverted light microscope (Leica DMI 4000 B; 20×). To analyze plaque sizes and morphology, OFTu cells were cultured in six-well plates inoculated with serial 10-fold dilutions of each virus (10^{-4} to 10^{-6}) and fixed with 3.7% formaldehyde, 72 h p.i. Cells were stained with 1% crystal violet for 15 min at room temperature, and plaques were examined under an inverted microscope (Leica DMI 4000 B; 20×).

Microarray and real-time PCR analysis. Gene expression profile of virus-infected OFTu cells was initially analyzed by microarray and then confirmed by real-time PCR. OFTu cells grown in 35 mm dishes for 16 h at 37°C with 5% of CO_2 were inoculated with wild-type or mutant virus (MOI = 10) and harvested for total RNA extraction with TRIzol reagent (Invitrogen, San Diego, CA) at 2 and 4 h p.i.

For microarray analysis, RNA samples were processed and prepared according to standard Affymetrix protocols (Santa Clara, CA) at the Biotechnology Center of the University of Illinois at Urbana-Champaign. The gene expression profile at each time point was measured by using the Affymetrix GeneChip Bovine Genome Array which contains 24,128 probe sets that measure over 23,000 bovine transcripts. After the data passed the Affymetrix's recommended quality control, arrays were preprocessed by using the GCRMA algorithm (68) as part of the Affymetrix (23) and GCRMA (68) packages from the Bioconductor project (25). Fold changes in gene expression were calculated for each time point by comparing expression in cells infected with the mutant virus with those infected by wild-type virus.

Real-time PCR was performed to validate the microarray results. One microgram of total RNA, obtained from samples of three independent experiments, was used for cDNA synthesis as described above. Expression of genes CCL20, CXCL3, IL-1α, IL-6, IL-8, ICAM-1, IRF-1, NFκBIA, and PTGS2 was analyzed in an ABI Prism 7900HT (Applied Biosystems, Foster City, CA). Primers and probes used to detect the expression of these genes were synthesized by Applied Biosystems (TaqMan gene expression custom assays), based on ovine gene sequences in GenBank. Real-time PCR amplifications were performed in 10-μl reactions, with 4.5 μl of cDNA (1:80 dilution in diethyl pyrocarbonate-H_2O), 5 μl of TaqMan Master mix (Applied Biosystems), and 0.5 μl of the mixture of primers and probe (TaqMan gene expression custom assays). PCR conditions consisted of initial denaturation and DNA polymerase activation (Ampli*Taq* Gold, Applied Biosystems) at 95°C for 15 s, followed by annealing and extension at 60°C for 1 min.

Each sample was tested in triplicate and the average of the three replicates was used to calculate fold changes. Expression levels of the genes tested were normalized to the housekeeping gene GAPDH (glyceraldehyde-3-phosphate dehydrogenase). The measurement of gene expression was performed by using the relative quantitation method (67). Standard curves were prepared from a pool of cDNA (2-fold dilutions; 1:20 to 1:2,560) for GAPDH and all tested genes. Samples from mock-infected cells collected at 2 and 4 h p.i. were used as calibrators to calculate the fold changes. Negative controls (no template) and controls for DNA contamination (no RT control) were included in all reactions. Statistical analysis of the real-time PCR data was performed by using a Student *t* test.

Establishment of cell lines stably expressing ORFV024. HeLa cells constitutively expressing green fluorescent protein (GFP) or ORFV024-GFP fusion protein were obtained by using a retroviral expression system (pLNCX2; Clontech). DNA sequences encoding GFP or ORFV024-GFP were cleaved from vectors pEGFP-N1 and p024EGFP with BglII and NotI and subcloned into plasmid pLNCX2. Plasmid constructs were transfected into the packaging cell lines GP2-293 using Lipofectamine 2000. At 48 h after transfection, the supernatant containing GFP- or ORFV024-GFP-encoding recombinant retrovirus particles was harvested and used to infect HeLa cells. Individual cell clones were selected, amplified, and maintained in the presence of G418 (500 μg/ml; Gibco). The expression of GFP and ORFV024-GFP was monitored by fluorescence microscopy and by Western immunoblot with an anti-GFP antibody (sc-8334; Santa Cruz Biotechnology, Santa Cruz, CA).

NF-κB luciferase reporter assays. The ability of ORFV024 to inhibit NF-κB-transcriptional activity was investigated *in vitro* using a luciferase reporter assay. OFTu cells were cultured in 12-well plates (1.2×10^5 cells per well) and co-transfected the next day with the vectors pNF-κB*Luc* (450 ng; Clontech, Mountain View, CA) and pRLTK (50 ng; Promega, Madison, WI), which encode the firefly luciferase gene under the control of κB-responsive elements and sea pansy (*Renilla reniformis*) luciferase, respectively, using Lipofectamine 2000 (Invitrogen). At 24 h after transfection, cells were mock infected or infected with wild-type (OV-IA82) or mutant virus (OV-IA82Δ024) (MOI = 10). Cells were harvested with passive lysis buffer at 2, 4, and 6 h p.i. (PLB; Promega), and luciferase activities were determined using a dual luciferase reporter assay (Promega) and a luminometer (Victor^2; Perkin-Elmer, Waltham, MA).

OFTu cells transiently expressing or HeLa cells stably expressing ORFV024 were cotransfected with the reporter plasmids, treated with LPS or TNF-α, respectively, and assayed for firefly and sea pansy luciferase activities. OFTu cells cultured in 12-well plates (1.2×10^5 cells per well) were cotransfected with pNF-κB*Luc* (450 ng), pRLTK (50 ng), and pCMV024-Flag (500 ng), or control empty vector pCMVTag4A (500 ng), using Lipofectamine 2000. At 24 h after transfection, cells were exposed to control media or media containing LPS (250 ng/ml; Invivogen, San Diego, CA) for 6 h. LPS-treated and untreated cells were harvested with PLB, and luciferase activity was determined as described above. HeLa cells stably expressing GFP or ORFV024-GFP fusion protein were cultured in 12-well plates (1.1×10^5 cells per well) and cotransfected with pNF-κB*Luc* (450 ng) and pRLTK (50 ng) as described above. At 24 h after transfection, cells were exposed to control media or media containing 20 or 50 ng of TNF-α (Cell Signaling, Danvers, MA)/ml for 6 h and assayed for firefly and sea pansy luciferase activities as described above. All transfections were performed in triplicate. Luciferase activities were measured as relative light units (RLU), and firefly luciferase was normalized to the sea pansy luciferase activity to correct for transfection efficiencies. Resultant ratios were used to calculate fold changes in the luciferase activity between control and treated cells. Statistical analysis of the data was performed by using Student's *t* test.

Western blots. Western immunoblots were used to assess the effect of ORFV024 expression on the NF-κB pathway. HeLa cells stably expressing GFP (GFP/HeLa) or ORFV024-GFP (024GFP/HeLa) were cultured in six-well plates for 48 h, treated with TNF-α (20 ng/ml, Cell Signaling), harvested at various times after TNF-α-treatment (at 5, 10, and 20 min or at 10 and 20 min), and lysed with ProteoJET mammalian lysis buffer (Fermentas, Glen Burnie, MD) containing protease and phosphatase inhibitors (Sigma-Aldrich, St. Louis, MO). OFTu cells cultured in six-well plates were transfected with pCMVTag4A (2 μg; control) or with pCMV024-Flag (2 μg) and, 24 h after transfection, treated with TNF-α (20 ng/ml; Cell Signaling), and harvested at 10 and 20 min after TNF-α treatment as described above. Untreated cells were used as controls in all experiments. Approximately 50 μg of total protein lysate were resolved by SDS-PAGE in 10% acrylamide gels, followed by blotting to nitrocellulose membranes (Bio-Rad). Blots were incubated overnight at 4°C with antibodies against IKKα (sc-52932; Santa Cruz), IKKβ (catalog no. 2370; Cell Signaling), phospho-IKKα/β (catalog no. 2681; Cell Signaling), IκBα (sc-371; Santa Cruz), phospho-IκBα (Ser32/36) (catalog no. 9246; Cell Signaling), NF-κB-p65 (sc-7151; Santa Cruz), phospho-NF-κB-p65 (Ser536) (catalog no. 3033; Cell Signaling), Gβ (sc-378; Santa Cruz), GAPDH (sc-25778; Santa Cruz), Flag-M2 (catalog no. 200471; Stratagene), or GFP (sc-8334; Santa Cruz). After washing to remove unbound antibodies (three times for 10 min with TBS-Tween 20 0.1%), blots were incubated with secondary goat anti-rabbit IgG-(HRP) (sc-2004; Santa Cruz) or goat

anti-mouse IgG-(HRP) (catalog no. 7076; Cell Signaling) for 1.5 h at room temperature and developed using chemiluminescent reagents (ECL; Pierce-Thermo Scientific, Rockford, IL). Densitometric analysis of the blots was performed by using the software ImageJ, version 1.62 (National Institutes of Health, Bethesda, MD). Statistical analysis of the densitometry data was performed by using Student *t* test.

Nuclear translocation of NF-κB-p65. Nuclear translocation of NF-κB-p65 was investigated in cells stably expressing GFP (GFP/HeLa) or ORFV024-GFP (024GFP/HeLa). Cells were cultured in six-well plates for 48 h (5×10^5 cells/well), treated with TNF-α (20 ng/ml) for 45 min and harvested in phosphate-buffered saline (PBS; 0.5 ml/well). Cytoplasmic and nuclear protein fractions were extracted by using a ProteoJet cytoplasmic and nuclear protein extraction kit (Fermentas, Glen Burnie, MD), after the manufacturer's protocol. Levels of translocated NF-κB-p65 were determined by western immunoblots as described above. A total of 20 μg of cytoplasmic and nuclear protein extracts were resolved by SDS-PAGE and blotted to nitrocellulose membranes. Blots were incubated with antibodies against NF-κB-p65 (sc-7151; Santa Cruz), GAPDH (sc-25778; Santa Cruz), or histone H3 (sc-10809; Santa Cruz) and detected with a secondary goat anti-rabbit-IgG-HRP antibody, followed by incubation with enhanced chemiluminescence (ECL) substrate.

Animal inoculation. Four to five-month-old lambs (70 to 80 lbs) were obtained from an orf-free flock and randomly allocated to three groups, consisting of mock-infected (MEM; $n = 3$), OV-IA82-infected ($n = 3$), and OV-IA82Δ024-infected lambs ($n = 3$). Lambs were tranquilized with xylazine (Rompun; Bayer), and sites of inoculation were cleaned with sterile water. Inoculation was performed by scarification of the mucocutaneous junction of the inferior lip, and the left axillary skin, followed by local application of 0.5 ml of virus suspension containing $10^{7.5}$ $TCID_{50}$/ml in MEM. Animals were monitored daily for 19 days for changes in body temperature and presence of mucocutaneous lesions, including erythema, papules, vesicles, pustules, and scabs. Skin biopsies were collected from the axilla on days 3, 5, 7, and 19 p.i. and processed for histological examination according to standard procedures. All animal procedures were reviewed and approved by the University of Nebraska-Lincoln Institutional Animal Care and Use Committee (protocol 08-01-001D of 01/22/08).

RESULTS

Parapoxvirus *ORF024* encodes for a novel protein with no homology to other viral or cellular proteins. ORFV and BPSV ORF024 are 288 to 292 amino acids and 227 amino acids in length, respectively, with predicted molecular masses ranging from 26.2 to 32.7 kDa. ORFV strain OV-IA82 ORFV024 shares 93 to 98%, 92%, and 62% amino acid identity with homologues from the sheep isolated ORFV strains OV-NZ2 and OV-Orf11, the goat isolated ORFV strain OV-SA00, and the BPSV strains BV-AR02 and BV-TX09, respectively. No homologues of ORFV024 were detected outside the parapoxviruses. Notably, whereas retaining residues 1 to 4 and residues 12 to 19, BPSV ORF024 lacks 64 residues present in the amino terminus of all ORFV strains. Although ORF024 carboxyl terminus is highly conserved among ORFV and BPSV strains, some degree of interspecies variability was observed at amino acid residues 116 to 132, 193 to 201, and 274 to 283. No motifs indicative of protein function were detected in ORFV024.

***ORFV024* is transcribed as an early gene and the protein localizes to the cell cytoplasm.** To determine the kinetics of *ORFV024* transcription, primary OFTu cells were inoculated with OV-IA82 in the presence or absence of AraC and cells were harvested at various times p.i. Transcription of *ORFV024* was detected by RT-PCR as early as 1 h p.i., and the levels of expression increased thereafter during the infection cycle (up to 24 h p.i.) either in the presence or absence of AraC (Fig. 1A). A similar transcription pattern was observed for the early ORFV gene *ORFV127* (Fig. 1A) (20). In contrast, transcription of *ORFV055*, which encodes for a late virion membrane protein (14) was detected at late times p.i. but was markedly decreased in AraC-treated cells (Fig. 1A). These results indicate that *ORFV024* belongs to the early class of poxviral genes, which is known to encode for proteins involved in immune evasion and immunomodulation (1).

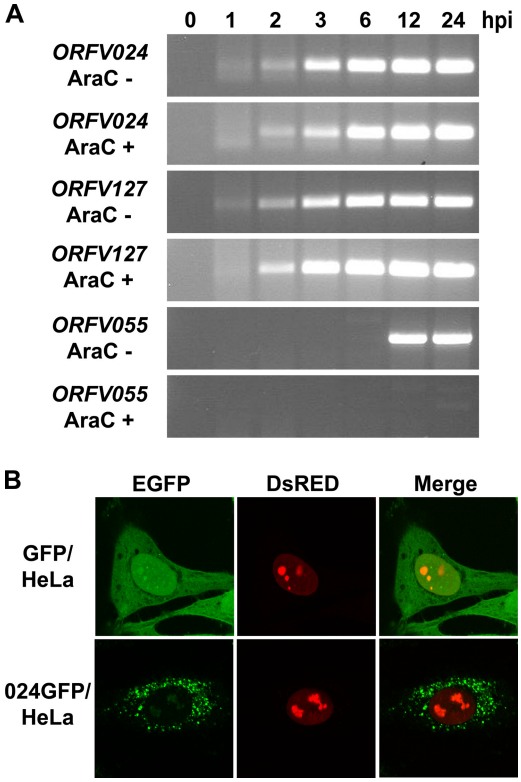

FIG. 1. Transcription kinetics and subcellular localization of ORFV024. (A) Transcription kinetics of *ORFV024*, *ORFV127*, and *ORFV055* during ORFV infection cycle in OFTu cells in the presence or absence of AraC as determined by RT-PCR. (B) ORFV024 punctate localization in the cytoplasm of 024GFP/HeLa stable cell lines.

The subcellular localization of ORFV024 was investigated in HeLa cells stably expressing ORFV024-GFP fusion protein. ORFV024 localized to the cell cytoplasm, exhibiting a punctate distribution pattern in this compartment (Fig. 1B). A similar distribution pattern of ORFV024-GFP was observed in stable cell lines infected with OV-IA82Δ024 (data not shown). No colocalization was detected when 024GFP/HeLa cells were transfected with plasmids encoding for markers for the nucleus (pDSRed-Nuc) (Fig. 1B), endoplasmic reticulum (pDSRed-ER), mitochondria (pDSRed-Mito), or peroxisomes (pDSRed-Peroxi) (data not shown). ORFV024 was similarly distributed in OFTu cells transiently expressing ORFV024-GFP fusion protein (data not shown).

Construction and characterization of *ORFV024* deletion mutant virus OV-IA82Δ024. Using homologous recombination, *ORFV024* was deleted from the OV-IA82 genome and recombinant viruses were selected, and plaque purified in the presence of X-Gluc. Deleted gene sequences were not detected in samples from cells infected with recombinant virus. In contrast, β-glucuronidase sequences were detected in DNA samples from cells infected with recombinant but not wild-type virus (data not shown). DNA sequencing of

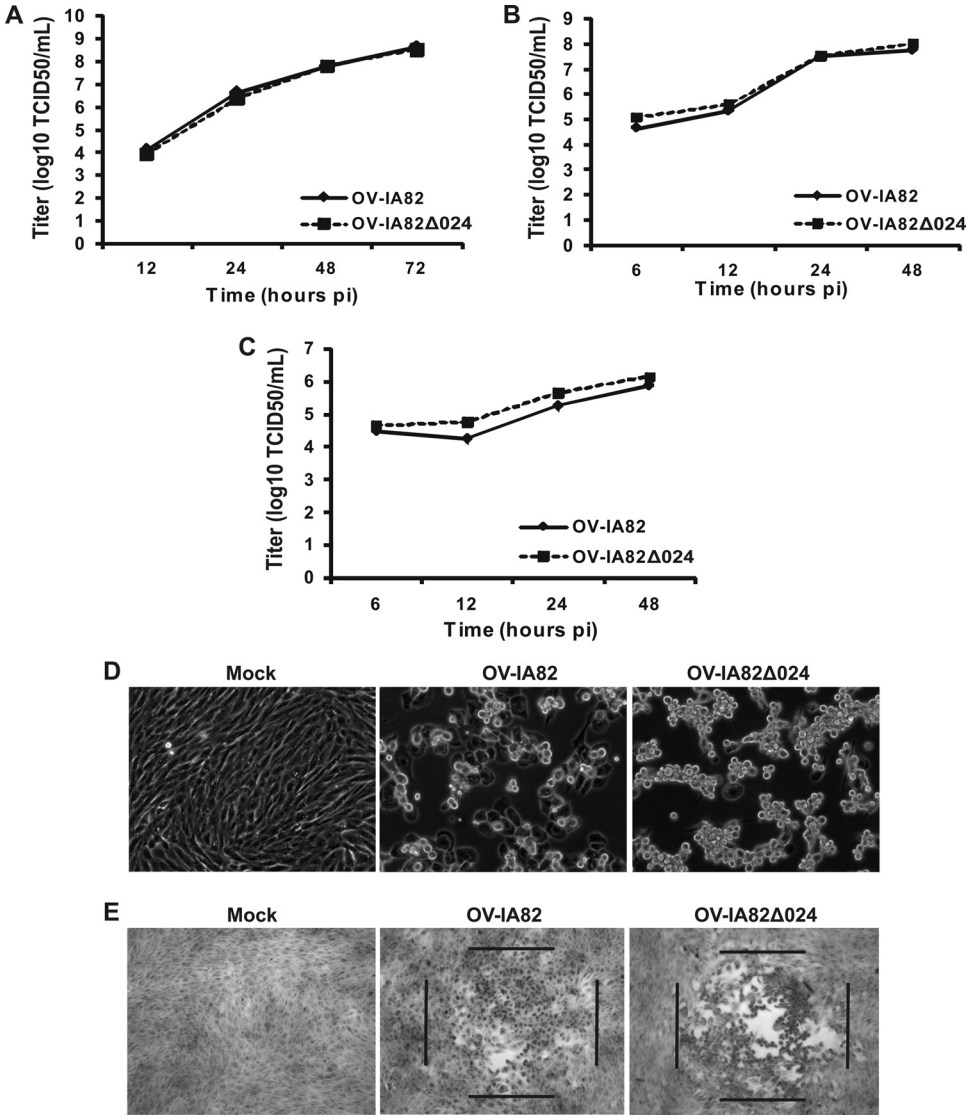

FIG. 2. Growth characteristics of *ORFV024* deletion mutant virus OV-IA82Δ024. (A) Multiple step growth curves of wild-type and mutant virus in primary OFTu cells. One-step growth curves of wild-type and mutant virus in primary OFTu (B) and in HeLa cells (C). (D) CPE of wild-type and mutant virus in primary OFTu cells 48 h after infection (MOI = 10) (magnification, ×20). (E) Plaque morphology of wild-type and mutant viruses in OFTu cells. At 72 h after infection cells were fixed with formaldehyde (3.7%) and stained with 1% crystal violet (magnification, ×20). Black bars demarcate plaques produced by OV-IA82 and OV-IA82Δ024.

regions flanking the deleted gene confirmed the integrity of parental virus sequences in the mutant virus (data not shown).

***ORFV024* is nonessential for ORFV replication *in vitro* but affects CPE and plaque morphology.** Replication properties of OV-IA82Δ024 and OV-IA82 were compared after infection of primary OFTu cells and HeLa cells. No significant differences in replication kinetics and viral yields were detected between wild-type and mutant virus either in OFTu or in HeLa cells, indicating that *ORFV024* is nonessential for ORFV replication in these cells (Fig. 2A, B, and C). Cytopathic effect (CPE) and plaque morphology induced by wild-type and mutant virus differed in OFTu-infected cells. While CPE induced by OV-IA82 was characterized by enlargement and flattening of infected cells, followed by cell rounding (Fig. 2D), CPE induced by OV-IA82Δ024 was characterized by cell rounding, followed by arrangement of cells in grapelike clusters, and absence of enlarged flattened cells (Fig. 2D). Although the plaques produced by wild-type and mutant virus were of similar size, OV-IA82Δ024 plaques exhibited a distinct morphology (Fig. 2E). OV-IA82 plaques consisted of large flat cells around a small cell-free central area, whereas OV-IA82Δ024 plaques were characterized by a large cell-free central area and absence of flattened cells (Fig. 2E).

OV-IA82Δ024 infection results in an increased expression of NF-κB-regulated genes in primary OFTu cells. To investigate potential function(s) for ORFV024 during ORFV infection, microarray analysis was performed to determine the profile of gene expression in OFTu cells infected with wild-type or *ORFV024* deletion mutant virus. Cells infected with OV-

TABLE 1. Summary of NF-κB-regulated genes detected by microarray and real-time PCR in primary OFTu cells infected with OV-IA82 or *ORFV024* deletion mutant virus OV-IA82Δ024

Gene	Description	GenBank	mRNA expression detected by:					
			Microarray analysis of OFTu cells infected with OV-IA82Δ024[a]		Real-time PCR in OFTu cells infected with OV-IA82 or OV-IA82Δ024[b]			
					2 h p.i.		4 h p.i.	
			2 h p.i.	4 h p.i.	OV-IA82	OV-IA82Δ024	OV-IA82	OV-IA82Δ024
CCL20	Chemokine ligant 20	NM_174263	80.02	205.16	1.02 ± 0.11	42.68 ± 6.17*	0.43 ± 0.03	38.21 ± 4.05*
CXCL1	Chemokine ligant 1	NM_175700	73.72	1.75	–	–	–	–
CXCL2	Chemokine ligant 2	NM_174299	69.95	7.10	–	–	–	–
CXCL3	Chemokine ligant 3	NM_001046513	7.27	12.34	0.71 ± 0.07	49.5 ± 6.34*	1.49 ± 0.13	20.14 ± 4.85*
ICAM1	Intercellular adhesion molecule (CD54)	NM_174348	3.29	3.29	0.92 ± 0.08	3.98 ± 0.07†	0.73 ± 0.08	2.66 ± 0.30*
IL-1α	IL-1α	NM_174092	70.09	1.05	0.87 ± 0.06	27.79 ± 4.48*	0.75 ± 0.03	10.31 ± 1.52†
IL-6	IL-6	NM_173923	3.09	8.97	1.27 ± 0.37	7.60 ± 1.53*	0.70 ± 0.11	8.03 ± 0.12†
IL-8	IL-8	NM_173925	10.98	11.46	0.94 ± 0.03	26.65 ± 3.62*	0.61 ± 0.11	20.56 ± 1.69†
IRF1/LOC789216	IFN regulatory factor 1	NM_177432	17.01	1.00	0.89 ± 0.23	5.80 ± 0.38*	0.83 ± 0.1	1.14 ± 0.12
LOC614198	Similar to T-cell activation NF-κB like protein (TA-NF-κB)	XM_865597	7.23	1.00	–	–	–	–
MAIL	Molecule possessing ankyrin repeats induced by LPS	NM_174726	15.09	2.05	–	–	–	–
MGC142340	Similar to pentraxin-related protein PTX3 precursor	NM_001076259	5.98	7.52	–	–	–	–
MMP1	Matrix metallopeptidase 1 (intersticial collagenase)	NM_174112	3.01	4.91	–	–	–	–
MMP13	Matrix metallopeptidase 13 (collagenase 3)	NM_174398	1.70	2.88	–	–	–	–
MMP3	Matrix metallopeptidase 3 (progelatinase)	XM_586521	2.08	2.92	–	–	–	–
NFKBIA	Nuclear factor of kappa light polypeptidase gene enhancer in B-cell inhibitor, alpha	NM_001045868	9.12	4.40	0.92 ± 0.07	7.32 ± 0.93*	0.95 ± 0.08	3.4 ± 0.7*
PTGS2	Prostaglandin-endoperoxidase synthase 2	NM_17445	9.36	3.73	0.74 ± 0.10	8.44 ± 1.02†	0.59 ± 0.08	2.35 ± 0.64*

[a] Fold changes are relative to OFTu cells infected with the wild-type virus OV-IA82.
[b] Fold changes are relative to mock-infected OFTu cells, and the expression levels on those cells were equal to 1. Values are expressed as means calculated based on the mean expression levels of three independent experiments. –, Expression levels were not tested by real time-PCR. *, $P < 0.05$; †, $P < 0.01$.

IA82Δ024 exhibited a marked increase in expression of some chemokines and other proinflammatory genes (Table 1), most of which are known to be regulated by the NF-κB family of transcription factors (51). Notably, genes CCL20, CXCL1, CXCL2, IL-6, IL-8, NFκBIA, and PTGS2 were markedly upregulated (fold increases up to 205.1, 73.7, 69.9, 8.9, 11.4, 9.1, and 9.3, respectively) in OV-IA82Δ024-infected cells at 2 and 4 h p.i. (Table 1). The microarray data set was deposited in the Gene Expression Omnibus (GEO) database under the accession number GSE19415.

Microarray data were confirmed with real-time PCR, with all genes tested exhibiting increased expression in OV-IA82Δ024-infected cells (Table 1). No significant differences were observed between mock-infected and OV-IA82-infected cells (Table 1). These results indicate that expression of ORFV024 inhibits the transcription of NF-κB-regulated genes in wild-type virus-infected cells, likely by inhibiting the NF-κB signaling pathway.

Deletion of *ORFV024* from the OV-IA82 genome results in increased NF-κB-mediated gene transcription in infected cells. To investigate the effect of ORFV024 on NF-κB transcriptional activity, primary OFTu cells were transfected with a plasmid encoding a luciferase reporter gene under the control of a NF-κB-responsive promoter and subsequently inoculated with OV-IA82 or OV-IA82Δ024 or mock infected. Luciferase activity levels as determined at 2, 4, and 6 h p.i. were similarly low in mock-infected and in wild-type virus-infected cells. In contrast, infection with OV-IA82Δ024 resulted in a marked and significant increase of up to 5.8-fold ($P < 0.005$) in luciferase activity relative to mock-infected cells (Fig. 3A). These results indicate that expression of ORFV024 inhibits NF-κB-mediated gene transcription in ORFV-infected cells.

ORFV024 suppresses NF-κB-regulated gene transcription following treatment of cells with LPS and TNF-α. The ability of ORFV024 to inhibit NF-κB transcriptional activity was further investigated in primary OFTu and in HeLa cells. OFTu cells were cotransfected with a vector encoding for ORFV024-Flag fusion protein and with a plasmid encoding for a firefly luciferase reporter gene. Expression of ORFV024-Flag in LPS-treated OFTu cells significantly decreased NF-κB-regulated luciferase activity (~2-fold; $P < 0.01$) compared to control cells (Fig. 3B and C). Additionally, HeLa cells stably expressing GFP or ORFV024-GFP were transfected with the vector encoding the firefly luciferase reporter gene and treated with TNF-α for 6 h. NF-κB-mediated transcription of the luciferase gene was decreased approximately 4- to 5-fold ($P < 0.05$) in ORFV024-GFP-expressing cells compared to GFP-expressing controls (Fig. 3D and E). Together, these results indicate that ORFV024 inhibits activation of the NF-κB signaling pathway by two potent inducers, LPS and TNF-α.

ORFV024 decreases phosphorylation and nuclear translocation of NF-κB-p65 induced by TNF-α. Given that posttrans-

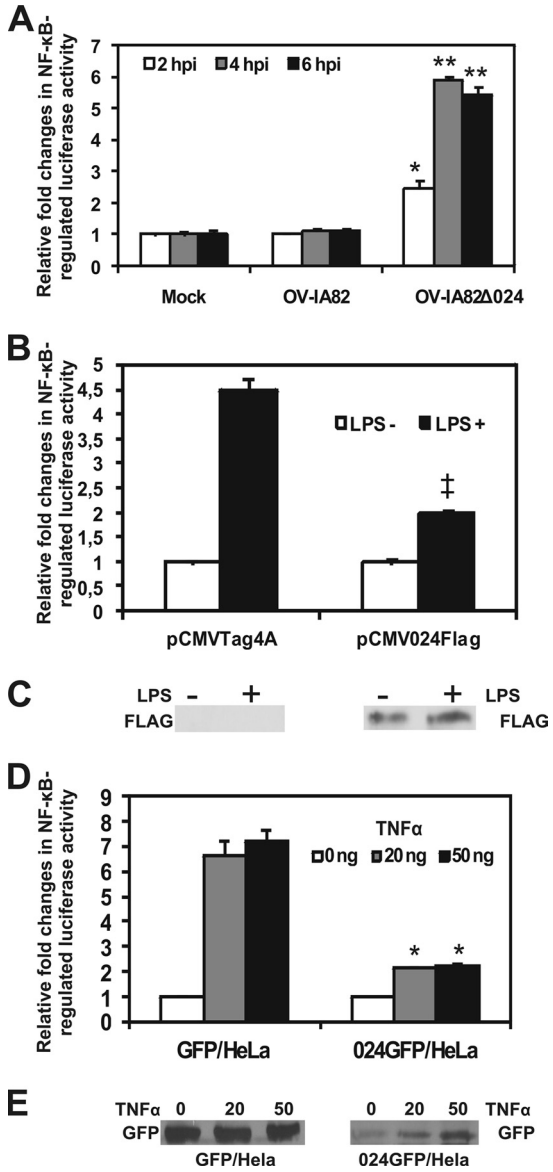

FIG. 3. Effect of ORFV024 on NF-κB-mediated transcription. (A) Primary OFTu cells were cotransfected with a vector encoding a firefly luciferase gene under the control of NF-κB (pNFκB-*Luc*) and with a plasmid encoding sea pansy (*Renilla reniformis*) luciferase under the control of herpesvirus TK promoter (pRL-TK). At 24 h after transfection cells were mock infected or infected with OV-IA82, or OV-IA82Δ024. Firefly and sea pansy luciferase activities were measured at 2, 4, and 6 h p.i. and expressed as relative fold changes in luciferase activity (⋆, $P < 0.05$; ⋆⋆, $P < 0.005$). (B) OFTu cells were cotransfected with pNFκB-*Luc*, pRL-TK, and pCMV024-Flag. At 24 h after transfection the cells were exposed to MEM containing 2% FBS and 0 or 250 ng of LPS/ml for 6 h. Cells were harvested, and firefly and sea pansy luciferase activities were measured and expressed as fold changes in luciferase activity (‡, $P < 0.01$). (C) Western blot analysis of cell lysates from samples tested in B (anti-Flag M2 antibody). (D) HeLa cells stably expressing GFP or ORFV024-GFP were cotransfected with pNFκB-*Luc* and pRL-TK. At 24 h after transfection, cells were exposed to MEM containing 2% FBS and 0, 20, or 50 ng of TNF-α/ml for 6 h. Cells were harvested, and the firefly and sea pansy luciferase activities were determined. Firefly luciferase activity was normalized to sea pansy luciferase activity and fold changes were calculated (⋆, $P < 0.05$). (E) Western blot analysis of cell lysates representative of samples tested in panel D (anti-GFP antibody). The results are representative of two (A and B) or three (D) independent experiments.

lational modifications define transcriptional functions of NF-κB-p65 in the nucleus (4, 36, 54), the effect of ORFV024 expression on NF-κB-p65 phosphorylation was investigated. HeLa cells stably expressing GFP (GFP/HeLa) or ORFV024-GFP (024GFP/HeLa) and OFTu cells transfected with pCMVTag4A (empty) or pCMV024-Flag were treated with TNF-α and harvested at various times posttreatment. The expression of ORFV024 markedly decreased phosphorylation of NF-κB-p65 at Ser536 induced by TNF-α in both HeLa and OFTu cells (Fig. 4A and C). Densitometric analysis of blots probed with phosphor-NF-κB-p65 (Ser536) antibody revealed reductions of 51 and 66% in the phosphorylation of NF-κB-p65 in HeLa and OFTu cells, respectively (Fig. 4B, $P < 0.005$; and Fig. 4D, $P < 0.05$). The reduced levels of phosphor-NF-κB-p65 are not due to protein degradation since levels of pan-NF-κB-p65 and Gβ were constant among all samples examined (Fig. 4A and C).

In addition, nuclear translocation of NF-κB-p65 in response to TNF-α treatment was assessed in cells stably expressing GFP (GFP/HeLa) or ORFV024-GFP (024GFP/HeLa). Expression of ORFV024-GFP markedly decreased nuclear translocation of NF-κB-p65 in response to TNF-α-treatment compared to control GFP-expressing cells (Fig. 4E). The decreased levels of NF-κB-p65 in the nucleus of 024GFP/HeLa cells were not due to protein degradation or to differences in protein loading, since levels of NF-κB-p65 in cell cytoplasm extracts were constant and no differences in the levels of the nuclear protein histone H3 were detected among the GFP and ORFV024-GFP samples. Together, the decreased levels of phosphor and nuclear translocated NF-κB-p65 demonstrate an inhibitory effect for ORFV024 on the NF-κB signaling pathway and further indicate the protein interferes with the pathway upstream of NF-κB-p65 phosphorylation.

ORFV024 decreases phosphorylation of IKKα and IKKβ in TNF-α-treated cells. The crucial step on the activation of NF-κB signaling pathway is the phosphorylation and subsequent degradation of IκBα, which leads to release, posttranslational modification, and nuclear translocation of NF-κB-p65 (33, 53). To investigate whether the decreased levels of phosphor and nuclear translocated NF-κB-p65 detected in ORFV024-expressing cells were due to an interference with IκBα phosphorylation and/or degradation, GFP/HeLa and 024GFP/HeLa cells were examined for pan and phosphor levels of IκBα. ORFV024 expression was accompanied by a decrease in TNF-α-induced IκBα phosphorylation and, consequently, its degradation (Fig. 5A). Densitometric analysis of blots probed with antibody against phosphor IκBα demonstrated a reduction of approximately 50% in IκBα phosphorylation in 024GFP/HeLa cells (Fig. 5B, $P < 0.005$).

IκB phosphorylation is mediated by upstream IκB kinases (33, 53). Given the importance of IKKs in triggering NF-κB activation and the decreased levels of phosphor IκBα detected in ORFV024-expressing cells, the potential role of ORFV 024 as an inhibitor of IKK activation was investigated. ORFV 024 expression markedly reduced phosphorylation of IKKα and IKKβ in 024GFP/HeLa cells (Fig. 6). These results indicate a role for ORFV024 in inhibiting IκBα phosphorylation and degradation by decreasing phosphorylation of IKK subunits IKKα/β.

ORFV024 is nonessential for ORFV virulence in the natural host. To investigate whether ORFV024 affects ORFV viru-

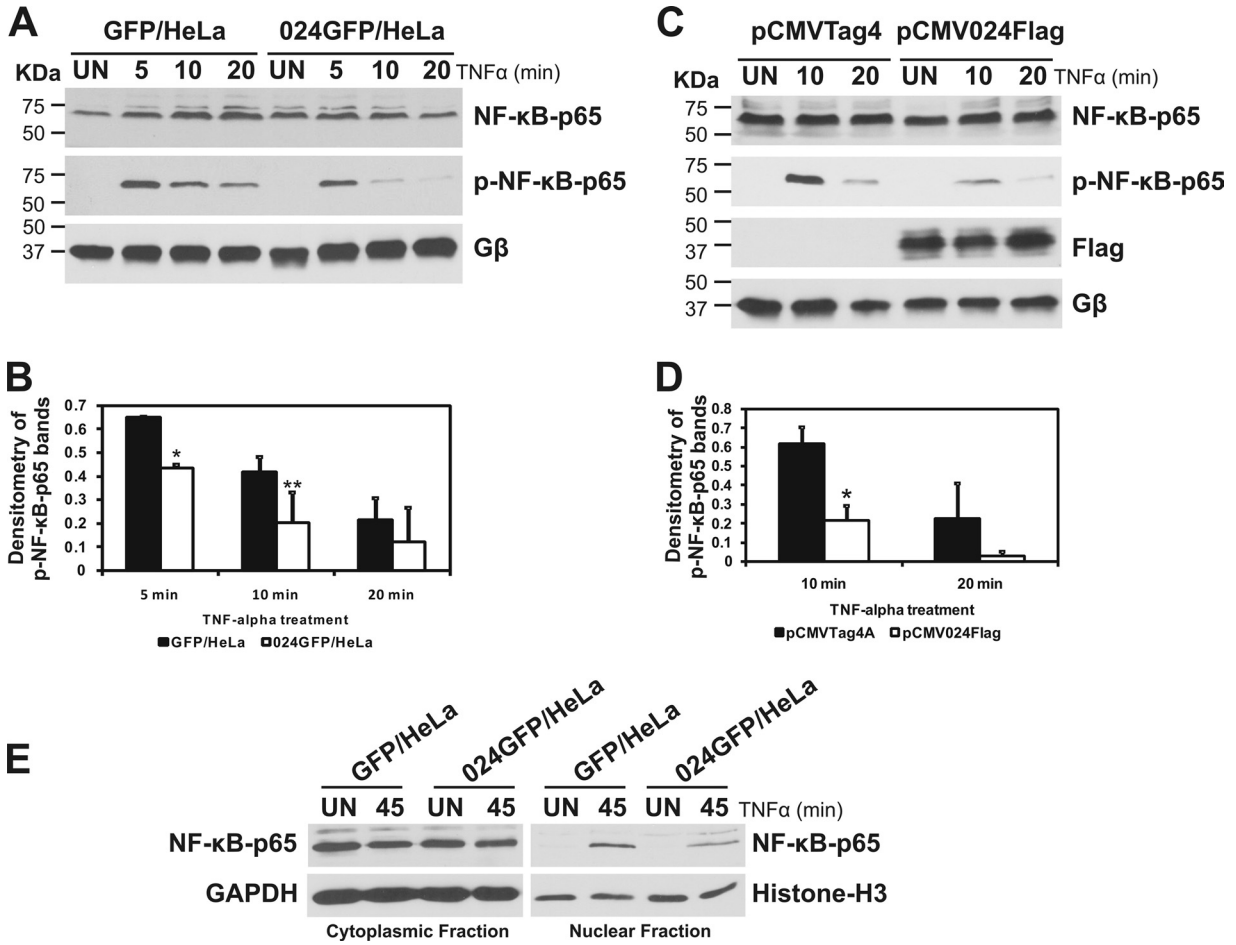

FIG. 4. Effect of ORFV024 expression on NF-κB-p65 phosphorylation and nuclear translocation. (A) HeLa cells stably expressing GFP (GFP/HeLa) or ORFV024-GFP (024GFP/HeLa) were treated with TNF-α (20 ng/ml) and harvested at the indicated times (UN, untreated controls). Fifty micrograms of total protein extracts were resolved by SDS-PAGE, blotted, and probed with antibodies against proteins indicated on the right. (B) Densitometry of phosphor NF-κB-p65 bands normalized to loading control Gβ (*, $P < 0.05$; **, $P < 0.005$). (C) OFTu cells were transfected with vectors pCMVTag4A (empty) or pCMV024-Flag, treated with TNF-α (20 ng/ml), and harvested at the indicated times (UN, untreated controls). Fifty micrograms of total protein extracts were resolved by SDS-PAGE, blotted, and probed with the antibodies directed against the proteins indicated on the right. (D) Densitometry of phosphor NF-κB-p65 bands normalized to loading control Gβ (*, $P < 0.05$). (E) HeLa cells stably expressing GFP (GFP/HeLa) or ORFV024-GFP (024GFP/HeLa) were treated with TNF-α (20 ng/ml) for 45 min, and cytoplasmic and nuclear protein fractions were extracted (UN, untreated controls). Twenty micrograms of total protein extracts were resolved by SDS-PAGE, blotted, and probed with antibodies against NF-κB-p65 (top panels), GAPDH (bottom left panel), or histone H3 (bottom right panel). The results are representative of two (E) or three independent experiments (A, B, C, and D).

lence, 4 to 5 months old, cross-breed lambs were inoculated with OV-IA82, OV-IA82Δ024, or MEM (control group). After local scarification, lambs were inoculated topically at the mucocutaneous junction of the lower lip and at the axillary skin and examined for the duration of the 19-day experiment. Characteristic clinical orf was observed in all virus-inoculated animals. Lesions developed by day 3 p.i. and consisted of erythema and papules, which evolved into vesicles and pustules at later times p.i. (Fig. 7). Local tissue proliferation and scab formation were first observed by days 5 and 7 p.i., respectively. Lesions started to subside on day 14 p.i. and by day 19 p.i. only limited scabs remained at lesion margins. No significant differences were observed in lesion severity, progression, or time to resolution between lambs inoculated with OV-IA82 or OV-IA82Δ024. Lambs from the control group did not exhibit changes other than mild scab formation due to skin scarification, which was completely resolved by day 4 p.i. (Fig. 7).

Histopathological changes in axillary skin from virus-inoculated lambs consisted of marked epidermal hyperplasia, ballooning degeneration of keratinocytes in the stratum spinosum, hyperkeratosis, dyskeratosis, dermal leukocyte infiltration, occasional intraepithelial microabscesses, and accumulation of scale-crust (data not shown). No significant differences in the severity or time course of histological changes were observed between lambs inoculated with OV-IA82 or OV-IA82Δ024. Samples from mock-inoculated lambs were indistinguishable from normal skin. These results indicate that ORFV024 does not significantly affect ORFV virulence in the natural host.

DISCUSSION

Microarray and real-time PCR analysis of cells infected with deletion mutant virus OV-IA82Δ024 indicated that ORFV024 suppresses expression of NF-κB regulated proinflammatory

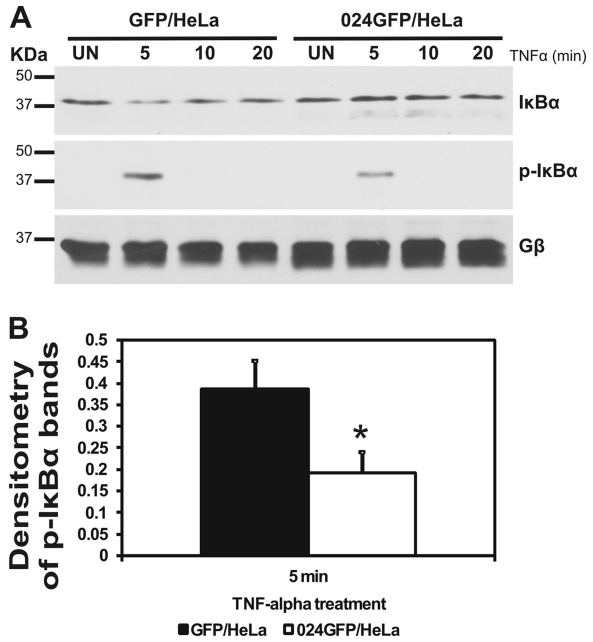

FIG. 5. Effect of ORFV024 expression on IκBα phosphorylation and degradation. (A) HeLa cells stably expressing GFP (GFP/HeLa) or ORFV024-GFP (024GFP/HeLa) fusion protein were treated with TNF-α (20 ng/ml) and harvested at the indicated times (UN, untreated controls). Fifty micrograms of total protein extracts were resolved SDS-PAGE, blotted, and probed with the antibodies directed against the proteins indicated on the right. (B) Densitometry of phosphor IκBα bands normalized to Gβ (*, $P < 0.005$). The results are representative of five independent experiments.

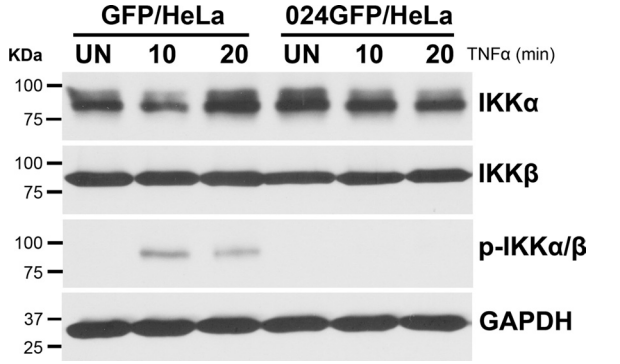

FIG. 6. Effect of ORFV024 expression on IKKα and IKKβ phosphorylation. HeLa cells stably expressing GFP (GFP/HeLa) or ORFV024-GFP (024GFP/HeLa) fusion protein were treated with TNF-α (20 ng/ml) and harvested at the indicated times (UN, untreated controls). Fifty micrograms of total protein extracts were resolved by SDS-PAGE, blotted, and probed with the antibodies against the proteins indicated on the right. The results are representative of three independent experiments.

genes, suggesting that ORFV024 inhibits activation of the NF-κB signaling pathway. Consistent with this hypothesis, we found a significant increase in expression of a NF-κB-responsive reporter gene in cells infected with OV-IA82Δ024 relative to those infected with wild-type virus. ORFV024 expression was shown here to suppress NF-κB-mediated transcription following treatment of cells with LPS or TNF-α. ORFV024 expression decreased TNF-α-induced phosphorylation and nuclear translocation of NF-κB-p65, phosphorylation and degradation of IκBα, and phosphorylation of IKK complex subunits IKKα and IKKβ. Together, these results indicate that ORFV024 prevents critical IKK activation, thus providing a mechanism for inhibition of NF-κB-mediated proinflammatory gene expression in infected cells.

Many poxviral proteins have been shown to inhibit activation of the IκB kinases, the bottleneck for most NF-κB-activating stimuli (11, 15, 24, 30, 45, 50, 62). For example, VACV proteins A46R, A52R, B14, and M2L interfere with activation of the IKK complex by antagonizing TLR signaling pathway (A46R and A52R), inhibiting activation of the IKK complex by the MEK/ERK signaling pathway (M2L), or directly binding to the IKK complex (B14L) (3, 11, 15, 24, 30, 62). In addition, VACV N1L presumably inhibits activation of the IKK complex by functioning upstream of IKKs, either at the level of adaptor protein TRAF6, or on downstream proteins that precede the IKK complex in the signaling cascade (26).

ORFV024 was shown here to inhibit activation of the IKK complex by decreasing phosphorylation of IKKα and IKKβ. Interaction of ORFV024 with IKKα, IKKβ, and IKKγ was investigated as a potential mechanism to prevent IκB kinase phosphorylation. However, no association between ORFV024 and IKKα, IKKβ, or IKKγ was detected (data not shown), suggesting that ORFV024 targets steps upstream of the IKK complex. Given that ORFV024 decreased expression of a NF-κB-responsive reporter gene following stimulation by both LPS and TNF-α, it is likely that this protein has evolved to interfere with activation of both, TLRs and TNFR signaling pathways (34, 65). The lack of homology between ORFV024 and other poxviral NF-κB inhibitors or any other molecule involved in the NF-κB signaling pathway, precludes assumptions on the precise mechanism by which ORFV024 interferes with IKK activation.

Like many poxviral genes encoding immune evasion and immunomodulatory proteins (1), including NF-κB inhibitors (42), transcription of *ORFV024* in cultured cells was detected throughout ORFV infection cycle, indicating that it belongs to the early class of viral genes (1). ORFV024-GFP fusion protein exhibited a punctate distribution in the cytoplasm of stably expressing cells, and no colocalization of ORFV024-GFP with markers for the nucleus and specific cellular organelles was observed. This is likely of biological significance given that NF-κB activation pathways affected by ORFV024 take place in the cell cytoplasm (reviewed by 33).

Replication characteristics of OV-IA82Δ024 in cultures of OFTu and HeLa cells were similar to those of OV-IA82, indicating that *ORFV024* is not essential for ORFV replication in these cells, and that like other poxviral NF-κB inhibitors (2, 11, 30, 41, 62), ORFV024 is dispensable for virus replication *in vitro*. Notably, OV-IA82Δ024 exhibited a distinct CPE (cell rounding and arrangement of cells in grapelike clusters) and plaque morphology (large cell-free central area and absence of flattened cells) in OFTu cells. These differences are likely explained by the increased expression of NF-κB-regulated genes induced by OV-IA82Δ024 infection, since activation of the NF-κB signaling pathway, and consequent gene expression, have been implicated in morphological and cytoskeletal

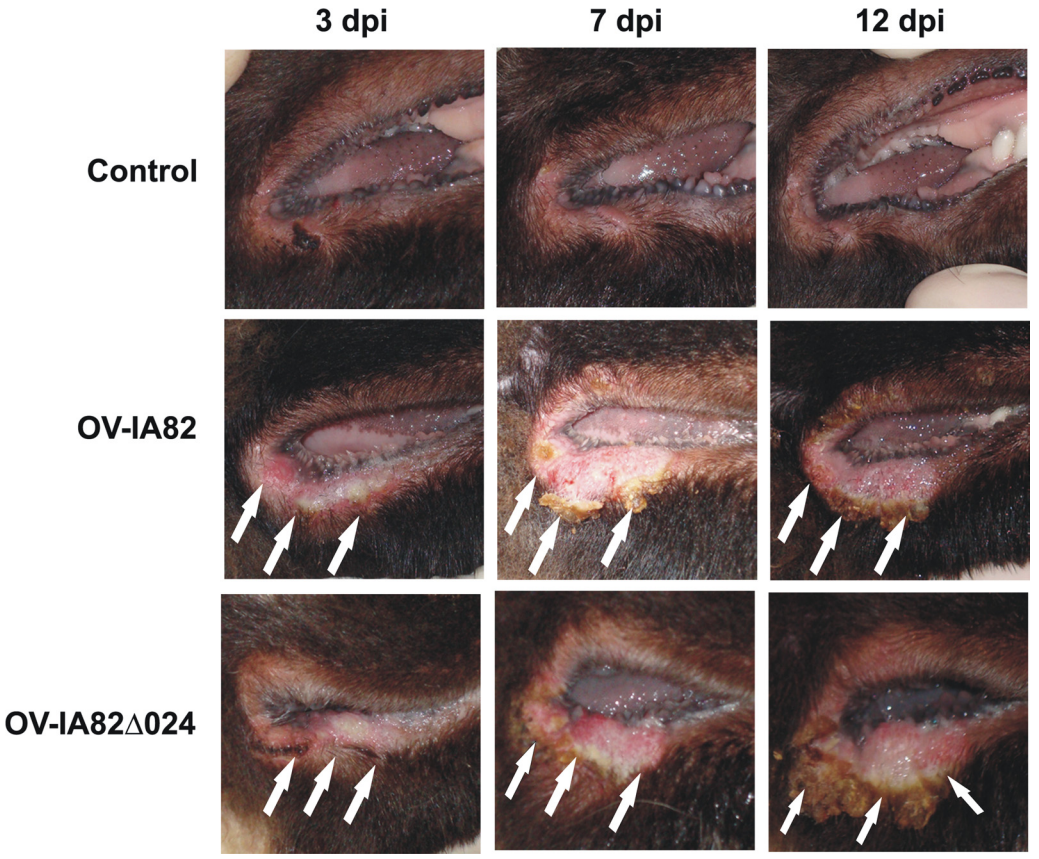

FIG. 7. Clinical course of orf in sheep. Groups of four- to five-month-old lambs were inoculated with MEM, OV-IA82, or OV-IA82Δ024 at the mucocutaneous border of the lower lip following scarification. Characteristic orf lesions (arrows) were observed in both OV-IA82 and OV-IA82Δ024 inoculated lambs (days 3, 7, and 12 p.i.).

changes in microglial cells after exposure to dsRNA (47) and in human endothelial cells expressing a viral activator of the NF-κB pathway (K13 protein from human herpesvirus 8) (37). The mechanisms by which ORFV024 influences cell morphology and cytoskeleton organization remain to be determined.

Given that the NF-κB signaling pathway integrates many aspects of the host innate and adaptive immunity (56), it was surprising that deletion of *ORFV024* from the OV-IA82 genome had no significant effect on disease severity, progression, and resolution in sheep, indicating that ORFV024 is nonessential for virus virulence in the natural host. Although selected poxviral NF-κB inhibitors have been shown to affect virus virulence and pathogenesis to some extent (2, 11, 30, 41, 62), the degree of attenuation after single viral gene deletions has been modest and variable. For example, VACV *B14R* was shown to contribute to virus virulence in an intranasal but not intradermal murine model of infection (10), while deletion of VACV *A46R*, *A52R*, or *N1L*, rendered the virus partially attenuated in a mouse intranasal model (2, 30). In contrast, deletion of ankyrin repeat-encoding myxoma virus *M150R* and cowpox virus *CPXV006* genes resulted in marked virus attenuation in rabbit intradermal and mouse intratracheal models of infection, respectively (6, 42). These observations indicate that the contribution of poxviral NF-κB inhibitors to virus infection and disease pathogenesis is complex and further suggest that multiple inhibitors encoded by individual poxviruses may exert complementary, perhaps partially overlapping functions to effectively evade NF-κB-mediated host immune responses.

The results presented here, showing that *ORFV024* deletion had no significant effect on ORFV pathogenesis in sheep, further support the possibility for complementary functions by poxviral NF-κB inhibitors during infections *in vivo*. Indeed, we have identified two additional ORFV-encoded genes that interfere with the NF-κB signaling pathway (unpublished data), suggesting that ORFV NF-κB inhibitors may function in a coordinated and complementary fashion on distinct branches of the NF-κB signaling cascade to effectively suppress NF-κB-mediated host immune responses *in vivo*. Given the potential complementary actions of multiple poxviral NF-κB inhibitors, single viral gene deletions may not result in significant effects on virus virulence and pathogenesis.

Alternatively, ORFV024 may function in other, less-understood aspects of host-ORFV interactions. For example, persistent and/or subclinical infections have been described for ORFV and BPSV (32, 49, 58). The high prevalence of antibodies against parapoxviruses in herds and flocks with no history of clinical infections (35; unpublished data) and the ability of ORFV to persist in a flock in the absence of clinical manifestation of infection (49) suggest that persistent or subclinical infections likely play a role in the maintenance of parapoxviruses in nature. It is tempting to speculate that ORFV NF-κB inhibitors such as ORFV024 may contribute to aspects of virus

persistence and transmission in the absence of overt viral infection.

The present study demonstrates that the novel ORFV protein ORFV024 interferes with activation of the NF-κB signaling pathway, while not significantly affecting virus virulence in the natural host. This represents the first description of an NF-κB inhibitor for ORFV or any other member of the *Parapoxvirus* genus. An improved understanding of ORFV functions associated with modulation and manipulation of host immune responses may contribute to increase current knowledge about the molecular aspects of ORFV biology and host-virus interactions.

ACKNOWLEDGMENTS

We thank T. Shors (Department of Biology and Microbiology, University of Wisconsin-Oshkosh), M. Varela and P. R. Murcia (Institute of Comparative Medicine, University of Glasgow Veterinary School, Glasgow, United Kingdom), D. Refojo (Max Planck Institute of Psychiatry, Munich, Germany), and J. Shisler (Department of Microbiology, University of Illinois) for providing plasmids used in the present study.

REFERENCES

1. **Assarsson, E., J. A. Greenbaum, M. Sundstrom, L. Schaffer, J. A. Hammond, V. Pasquetto, C. Oseroff, R. C. Hendrickson, E. J. Lefkowitz, D. C. Tscharke, J. Sidney, H. M. Grey, S. R. Head, B. Peters, and A. Sette.** 2008. Kinetic analysis of a complete poxvirus transcriptome reveals an immediate-early class of genes. Proc. Natl. Acad. Sci. U. S. A. **105:**2140–2145.
2. **Bartlett, N., J. A. Symons, D. C. Tscharke, and G. L. Smith.** 2002. The vaccinia virus N1L protein is an intracellular homodimer that promotes virulence. J. Gen. Virol. **83:**1965–1976.
3. **Bowie, A., E. Kiss-Toth, J. A. Symons, G. L. Smith, S. K. Dower, and L. A. O'Neill.** 2000. A46R and A52R from vaccinia virus are antagonists of host IL-1 and Toll-like receptor signaling. Proc. Natl. Acad. Sci. U. S. A. **97:**10162–10167.
4. **Buss, H., A. Dorrie, M. L. Schmitz, E. Hoffmann, K. Resch, and M. Kracht.** 2004. Constitutive and interleukin-1-inducible phosphorylation of p65 NF-κB at serine 536 is mediated by multiple protein kinases including IκB kinase (IKK)-alpha, IKKbeta, IKKepsilon, TRAF family member-associated (TANK)-binding kinase 1 (TBK1), and an unknown kinase and couples p65 to TATA-binding protein-associated factor II31-mediated interleukin-8 transcription. J. Biol. Chem. **279:**55633–55643.
5. **Buttner, M.** 1993. Principles of paramunization. Option and limits in veterinary medicine. Comp. Immunol. Microbiol. Infect. Dis. **16:**1–10.
6. **Camus-Bouclainville, C., L. Fiette, S. Bouchiha, B. Pignolet, D. Counor, C. Filipe, J. Gelfi, and F. Messud-Petit.** 2004. A virulence factor of myxoma virus colocalizes with NF-κB in the nucleus and interferes with inflammation. J. Virol. **78:**2510–2516.
7. **Castrucci, G., M. Ferrari, B. I. Osburn, F. Frigeri, F. Barreca, S. Tagliati, and V. Cuteri.** 1995. The use of a nonspecific defense mechanism inducer in calves exposed to bovine herpesvirus-1 infection: preliminary trials. Comp. Immunol. Microbiol. Infect. Dis. **18:**85–91.
8. **Chen, F., L. M. Demers, and X. Shi.** 2002. Upstream signal transduction of NF-κB activation. Curr. Drug Targets Inflamm. Allergy **1:**137–149.
9. **Chen, L. F., and W. C. Greene.** 2004. Shaping the nuclear action of NF-κB. Nat. Rev. Mol. Cell. Biol. **5:**392–401.
10. **Chen, R. A., N. Jacobs, and G. L. Smith.** 2006. Vaccinia virus strain Western Reserve protein B14 is an intracellular virulence factor. J. Gen. Virol. **87:**1451–1458.
11. **Chen, R. A., G. Ryzhakov, S. Cooray, F. Randow, and G. L. Smith.** 2008. Inhibition of IκB kinase by vaccinia virus virulence factor B14. PLoS Pathog. **4:**e22.
12. **Chisholm, S. E., and H. T. Reyburn.** 2006. Recognition of vaccinia virus-infected cells by human natural killer cells depends on natural cytotoxicity receptors. J. Virol. **80:**2225–2233.
13. **de la Concha-Bermejillo, A., J. Guo, Z. Zhang, and D. Waldron.** 2003. Severe persistent orf in young goats. J. Vet. Diagn. Invest. **15:**423–431.
14. **Delhon, G., E. R. Tulman, C. L. Afonso, Z. Lu, A. de la Concha-Bermejillo, H. D. Lehmkuhl, M. E. Piccone, G. F. Kutish, and D. L. Rock.** 2004. Genomes of the parapoxviruses ORF virus and bovine papular stomatitis virus. J. Virol. **78:**168–177.
15. **DiPerna, G., J. Stack, A. G. Bowie, A. Boyd, G. Kotwal, Z. Zhang, S. Arvikar, E. Latz, K. A. Fitzgerald, and W. L. Marshall.** 2004. Poxvirus protein N1L targets the I-κB kinase complex, inhibits signaling to NF-κB by the tumor necrosis factor superfamily of receptors, and inhibits NF-κB and IRF3 signaling by Toll-like receptors. J. Biol. Chem. **279:**36570–36578.
16. **Dvoracek, B., and T. Shors.** 2003. Construction of a novel set of transfer vectors to study vaccinia virus replication and foreign gene expression. Plasmid **49:**9–17.
17. **Erickson, G. A., E. A. Carbrey, and G. A. Gustafson.** 1975. Generalized contagious ecthyma in a sheep rancher: diagnostic considerations. J. Am. Vet. Med. Assoc. **166:**262–263.
18. **Fachinger, V., T. Schlapp, and A. Saalmuller.** 2000. Evidence for a parapox ovis virus-associated superantigen. Eur. J. Immunol. **30:**2962–2971.
19. **Fachinger, V., T. Schlapp, W. Strube, N. Schmeer, and A. Saalmuller.** 2000. Poxvirus-induced immunostimulating effects on porcine leukocytes. J. Virol. **74:**7943–7951.
20. **Fleming, S. B., D. M. Haig, P. Nettleton, H. W. Reid, C. A. McCaughan, L. M. Wise, and A. Mercer.** 2000. Sequence and functional analysis of a homolog of interleukin-10 encoded by the parapoxvirus orf virus. Virus Genes **21:**85–95.
21. **Fleming, S. B., and A. A. Mercer.** 2007. Genus *Parapoxvirus*, p. 127–165. *In* A. A. Mercer, A. Schmidt, and O. Weber (ed.), Poxviruses. Birkhäuser, Basel, Switzerland.
22. **Friebe, A., A. Siegling, S. Friederichs, H. D. Volk, and O. Weber.** 2004. Immunomodulatory effects of inactivated parapoxvirus ovis (ORF virus) on human peripheral immune cells: induction of cytokine secretion in monocytes and Th1-like cells. J. Virol. **78:**9400–9411.
23. **Gautier, L., L. Cope, B. M. Bolstad, and R. A. Irizarry.** 2004. Affy–analysis of Affymetrix GeneChip data at the probe level. Bioinformatics **20:**307–315.
24. **Gedey, R., X. L. Jin, O. Hinthong, and J. L. Shisler.** 2006. Poxviral regulation of the host NF-κB response: the vaccinia virus M2L protein inhibits induction of NF-κB activation via an ERK2 pathway in virus-infected human embryonic kidney cells. J. Virol. **80:**8676–8685.
25. **Gentleman, R. C., V. J. Carey, D. M. Bates, B. Bolstad, M. Dettling, S. Dudoit, B. Ellis, L. Gautier, Y. Ge, J. Gentry, K. Hornik, T. Hothorn, W. Huber, S. Iacus, R. Irizarry, F. Leisch, C. Li, M. Maechler, A. J. Rossini, G. Sawitzki, C. Smith, G. Smyth, L. Tierney, J. Y. Yang, and J. Zhang.** 2004. Bioconductor: open software development for computational biology and bioinformatics. Genome Biol. **5:**R80.
26. **Graham, S. C., M. W. Bahar, S. Cooray, R. A. Chen, D. M. Whalen, N. G. Abrescia, D. Alderton, R. J. Owens, D. I. Stuart, G. L. Smith, and J. M. Grimes.** 2008. Vaccinia virus proteins A52 and B14 Share a Bcl-2-like fold but have evolved to inhibit NF-κB rather than apoptosis. PLoS Pathog. **4:**e1000128.
27. **Guo, J., Z. Zhang, J. F. Edwards, R. W. Ermel, C. Taylor, Jr., and A. de la Concha-Bermejillo.** 2003. Characterization of a North American orf virus isolated from a goat with persistent, proliferative dermatitis. Virus Res. **93:**169–179.
28. **Haig, D. M., and C. J. McInnes.** 2002. Immunity and counter-immunity during infection with the parapoxvirus orf virus. Virus Res. **88:**3–16.
29. **Haig, D. M., and A. A. Mercer.** 1998. Ovine diseases. Orf. Vet. Res. **29:**311–326.
30. **Harte, M. T., I. R. Haga, G. Maloney, P. Gray, P. C. Reading, N. W. Bartlett, G. L. Smith, A. Bowie, and L. A. O'Neill.** 2003. The poxvirus protein A52R targets Toll-like receptor signaling complexes to suppress host defense. J. Exp. Med. **197:**343–351.
31. **Hiscott, J., T. L. Nguyen, M. Arguello, P. Nakhaei, and S. Paz.** 2006. Manipulation of the nuclear factor-κB pathway and the innate immune response by viruses. Oncogene **25:**6844–6867.
32. **Iketani, Y., Y. Inoshima, A. Asano, K. Murakami, S. Shimizu, and H. Sentsui.** 2002. Persistent parapoxvirus infection in cattle. Microbiol. Immunol. **46:**285–291.
33. **Karin, M., and Y. Ben-Neriah.** 2000. Phosphorylation meets ubiquitination: the control of NF-κB activity. Annu. Rev. Immunol. **18:**621–663.
34. **Kawai, T., and S. Akira.** 2007. Signaling to NF-κB by Toll-like receptors. Trends Mol. Med. **13:**460–469.
35. **Kuroda, Y., M. Yoshida, T. Shibahara, T. Matsui, T. Nakane, H. Hara, Y. Inoshima, and H. Sentsui.** 1999. An epidemic of parapoxvirus infection among cattle: isolation and antibody survey. J. Vet. Med. Sci. **61:**749–753.
36. **Lawrence, T., M. Bebien, G. Y. Liu, V. Nizet, and M. Karin.** 2005. IKKα limits macrophage NF-κB activation and contributes to the resolution of inflammation. Nature **434:**1138–1143.
37. **Matta, H., R. M. Surabhi, J. Zhao, V. Punj, Q. Sun, S. Schamus, L. Mazzacurati, and P. M. Chaudhary.** 2007. Induction of spindle cell morphology in human vascular endothelial cells by human herpesvirus 8-encoded viral FLICE inhibitory protein K13. Oncogene **26:**1656–1660.
38. **Mayr, A., M. Buttner, G. Wolf, H. Meyer, and C. Czerny.** 1989. Experimental detection of the paraspecific effects of purified and inactivated poxviruses. Zentralbl. Veterinarmed. B **36:**81–99.
39. **Mazur, C., and R. D. Machado.** 1989. Detection of contagious pustular dermatitis virus of goats in a severe outbreak. Vet. Rec. **125:**419–420.
40. **McKeever, D. J., D. M. Jenkinson, G. Hutchison, and H. W. Reid.** 1988. Studies of the pathogenesis of orf virus infection in sheep. J. Comp. Pathol. **99:**317–328.
41. **Mohamed, M. R., and G. McFadden.** 2009. NFκB inhibitors: strategies from poxviruses. Cell Cycle **8:**3125–3132.
42. **Mohamed, M. R., M. M. Rahman, A. Rice, R. W. Moyer, S. J. Werden, and**

G. McFadden. 2009. Cowpox virus expresses a novel ankyrin repeat NF-κB inhibitor that controls inflammatory cell influx into virus-infected tissues and is critical for virus pathogenesis. J. Virol. **83:**9223–9236.
43. **Moss, B.** 2007. Poxviruses: the viruses and their replication, p. 2905–2946. *In* D. M. Knipe and P. M. Howley (ed.), Fields virology, vol. 2. Wolters Kluwer Health/Lippincott/The Williams & Wilkins Co., Philadelphia, PA.
44. **Mourtada, I., M. Le Tourneur, J. Chevrant-Breton, and F. Le Gall.** 2000. Human orf and erythema multiforme. Ann. Dermatol. Venereol. **127:**397–399.
45. **Murao, L. E., and J. L. Shisler.** 2005. The MCV MC159 protein inhibits late, but not early, events of TNF-alpha-induced NF-κB activation. Virology **340:** 255–264.
46. **Myskiw, C., J. Arsenio, R. van Bruggen, Y. Deschambault, and J. Cao.** 2009. Vaccinia virus E3 suppresses expression of diverse cytokines through inhibition of the PKR, NF-κB, and IRF3 pathways. J. Virol. **83:**6757–6768.
47. **Nakamichi, K., M. Saiki, H. Kitani, Y. Kuboyama, K. Morimoto, M. Takayama-Ito, and I. Kurane.** 2007. Roles of NF-κB and MAPK signaling pathways in morphological and cytoskeletal responses of microglia to double-stranded RNA. Neurosci. Lett. **414:**222–227.
48. **Ndikuwera, J., G. O. Odiawo, E. A. Usenik, N. D. Kock, J. S. Ogaa, and R. Kuiper.** 1992. Chronic contagious ecthyma and caseous lymphadenitis in two Boer goats. Vet. Rec. **131:**584–585.
49. **Nettleton, P. F., J. A. Gilray, D. L. Yirrell, G. R. Scott, and H. W. Reid.** 1996. Natural transmission of orf virus from clinically normal ewes to orf-naive sheep. Vet. Rec. **139:**364–366.
50. **Nichols, D. B., and J. L. Shisler.** 2009. Poxvirus MC160 protein utilizes multiple mechanisms to inhibit NF-κB activation mediated via components of the tumor necrosis factor receptor 1 signal transduction pathway. J. Virol. **83:**3162–3174.
51. **Pahl, H. L.** 1999. Activators and target genes of Rel/NF-κB transcription factors. Oncogene **18:**6853–6866.
52. **Perkins, N. D.** 2007. Integrating cell-signalling pathways with NF-κB and IKK function. Nat. Rev. Mol. Cell. Biol. **8:**49–62.
53. **Perkins, N. D.** 2006. Post-translational modifications regulating the activity and function of the nuclear factor κB pathway. Oncogene **25:**6717–6730.
54. **Sakurai, H., H. Chiba, H. Miyoshi, T. Sugita, and W. Toriumi.** 1999. IκB kinases phosphorylate NF-κB p65 subunit on serine 536 in the transactivation domain. J. Biol. Chem. **274:**30353–30356.
55. **Sanchez, R. L., A. Hebert, H. Lucia, and J. Swedo.** 1985. Orf. A case report with histologic, electron microscopic, and immunoperoxidase studies. Arch. Pathol. Lab. Med. **109:**166–170.
56. **Santoro, M. G., A. Rossi, and C. Amici.** 2003. NF-κB and virus infection: who controls whom. EMBO J. **22:**2552–2560.
57. **Scheidereit, C.** 2006. IκB kinase complexes: gateways to NF-κB activation and transcription. Oncogene **25:**6685–6705.
58. **Sentsui, H., K. Murakami, Y. Inoshima, T. Shibahara, and Y. Yokomizo.** 1999. Isolation of parapoxvirus from a cow treated with interferon-gamma. Vet. Microbiol. **70:**143–152.
59. **Shisler, J. L., and X. L. Jin.** 2004. The vaccinia virus K1L gene product inhibits host NF-κB activation by preventing IκBα degradation. J. Virol. **78:**3553–3560.
60. **Siegemund, S., A. Hartl, H. von Buttlar, F. Dautel, R. Raue, M. A. Freudenberg, G. Fejer, M. Buttner, G. Kohler, C. J. Kirschning, T. Sparwasser, and G. Alber.** 2009. Conventional bone marrow-derived dendritic cells contribute to Toll-like receptor-independent production of alpha/beta interferon in response to inactivated parapoxvirus ovis. J. Virol. **83:**9411–9422.
61. **Smith, G. L.** 2007. Genus *Orthopoxvirus*: vaccinia virus, p. 1–45. *In* A. A. Mercer, A. Schmidt, and O. Weber (ed.), Poxviruses. Birkhäuser, Basel, Switzerland.
62. **Stack, J., I. R. Haga, M. Schroder, N. W. Bartlett, G. Maloney, P. C. Reading, K. A. Fitzgerald, G. L. Smith, and A. G. Bowie.** 2005. Vaccinia virus protein A46R targets multiple Toll-like-interleukin-1 receptor adaptors and contributes to virulence. J. Exp. Med. **201:**1007–1018.
63. **Unterholzner, L., and A. G. Bowie.** 2008. The interplay between viruses and innate immune signaling: recent insights and therapeutic opportunities. Biochem. Pharmacol. **75:**589–602.
64. **Weber, O., P. Knolle, and H. D. Volk.** 2007. Immunomodulation by inactivated *Orf virus* (ORFV): therapeutic potential, p. 297–310. *In* A. A. Mercer, A. Schmidt, and O. Weber (ed.), Poxviruses. Birkhäuser, Basel, Switzerland.
65. **Wertz, I. E., and V. M. Dixit.** 2008. Ubiquitin-mediated regulation of TNFR1 signaling. Cytokine Growth Factor Rev. **19:**313–324.
66. **Westphal, D., E. C. Ledgerwood, M. H. Hibma, S. B. Fleming, E. M. Whelan, and A. A. Mercer.** 2007. A novel Bcl-2-like inhibitor of apoptosis is encoded by the parapoxvirus ORF virus. J. Virol. **81:**7178–7188.
67. **Wong, M. L., and J. F. Medrano.** 2005. Real-time PCR for mRNA quantitation. Biotechniques **39:**75–85.
68. **Wu, Z., and R. A. Irizarry.** 2005. Stochastic models inspired by hybridization theory for short oligonucleotide arrays. J. Comput. Biol. **12:**882–893.
69. **Yirrell, D. L., H. W. Reid, M. Norval, and S. E. Howie.** 1989. Immune response of lambs to experimental infection with Orf virus. Vet. Immunol. Immunopathol. **22:**321–332.
70. **Ziebell, K. L., H. Steinmann, D. Kretzdorn, T. Schlapp, K. Failing, and N. Schmeer.** 1997. The use of Baypamun N in crowding associated infectious respiratory disease: efficacy of Baypamun N (freeze-dried product) in 4-10 month old horses. Zentralbl. Veterinarmed. B **44:**529–536.